Perilipin 5, a lipid droplet-associated protein, provides physical and metabolic linkage to mitochondria[S]

Hong Wang,* Urmilla Sreenivasan,*,†Hong Hu,* Andrew Saladino, Brian M. Polster,[§] Linda M. Lund,*** Da-wei Gong,*,† William C. Stanley,*** and Carole Sztalryd[1,*,†]**

The Geriatric Research, Education and Clinical Center,* Baltimore Veterans Affairs Health Care Center, Division of Endocrinology,† Department of Medicine, School of Medicine, University of Maryland, Baltimore, Maryland 21201; VAMHCS Blood/Tissue Banks and Hematology,** Division of Pathology, Department of Medicine, School of Medicine, University of Maryland, Baltimore, Maryland 21201; Department of Anesthesiology and the Shock, Trauma and Anesthesiology Research (STAR) Center,[§] University of Maryland School of Medicine, University of Maryland, Baltimore, Maryland 21201; and Department of Medicine,*** Department of Physiology, School of Medicine, University of Maryland, Baltimore, Maryland 21201

Abstract Maintaining cellular lipid homeostasis is crucial to oxidative tissues, and it becomes compromised in obesity. Lipid droplets (LD) play a central role in lipid homeostasis by mediating fatty acid (FA) storage in the form of triglyceride, thereby lowering intracellular levels of lipids that mediate cellular lipotoxicity. LDs and mitochondria have interconnected functions, and anecdotal evidence suggests they physically interact. However, the mechanisms of interaction have not been identified. Perilipins are LD-scaffolding proteins and potential candidates to play a role in their interaction with mitochondria. We examined the contribution of LD perilipin composition to the physical and metabolic interactions between LD and mitochondria using multiple techniques: confocal imaging, electron microscopy (EM), and lipid storage and utilization measurements. Using neonatal cardiomyocytes, reconstituted cell culture models, and rodent heart tissues, we found that perilipin 5 (Plin5) recruits mitochondria to the LD surface through a C-terminal region. Compared with control cells, Plin5-expressing cells show decreased LD hydrolysis, decreased palmitate β-oxidation, and increased palmitate incorporation into triglycerides in basal conditions, whereas in stimulated conditions, LD hydrolysis inhibition is lifted and FA released for β-oxidation. These results suggest that Plin5 regulates oxidative LD hydrolysis and controls local FA flux to protect mitochondria against excessive exposure to FA during physiological stress.—Wang, H., U. Sreenivasan, H. Hu, A. Saladino, B. M. Polster, L. M. Lund, D. Gong, W. C. Stanley, and C. Sztalryd. **Perilipin 5, a lipid droplet-associated protein, provides physical and metabolic linkage to mitochondria. *J. Lipid Res.* 2011.** 52: **2159–2168.**

Supplementary key words perilipins • fatty acid β-oxidation • fluorescence microscopy • lipid droplets • lipids/efflux • mitochondria

Cellular energy homeostasis of oxidative tissue relies on a critical balance between fatty acid (FA) uptake from the environment and consumption by mitochondria oxidation. These processes are controlled by complex regulatory mechanisms that ensure energy needs are met while preventing buildup of toxic lipid intermediates and/or oxidized lipids. Transient formation of lipid droplets (LD) may protect mitochondria from lipotoxicity in physiological conditions such as fasting. However, with chronic excess FA levels as observed in obesity, LDs not only cease to be protective but may also contribute to pathology (1). Distinct features of cardiomyopathy appear in obese and diabetic type 2 patients, including accumulation of lipid droplets and long chain fatty acyl compounds (ceramides, acyl carnitines, and CoAs) in cardiomyocytes, which are

This work was supported by American Diabetes Association Career Development Award 1-05-CD-17 (C.S.); by National Institutes of Health Grant 1RO1-DK-075017 (C.S.); by American Heart Association Grant-in-Aid 11GRNT7600027 (C.S.); by the Geriatric Research, Education and Clinical Center of the Baltimore Veterans Affairs Health Care Center; by the Clinical Nutrition Research Unit of Maryland (DK-072488); and by the Intramural Research Programs of the National Institute of Diabetes and Digestive and Kidney Diseases (NIDDK) of the National Institutes of Health. Its contents are solely the responsibility of the authors and do not necessarily represent the official views of the National Institutes of Health. The costs of publication of this article were defrayed in part by the payment of page charges. This article must therefore be hereby marked "advertisement" in accordance with 18 U.S.C. Section 1734 solely to indicate this fact.

Manuscript received 16 June 2011 and in revised form 12 August 2011.

Published, JLR Papers in Press, August 31, 2011
DOI 10.1194/jlr.M017939

Abbreviations: AA, amino acid; ADFP, adipose differentiation-related protein; ASM, acid-soluble metabolite; CHO-K1, Chinese hamster ovary; EM, electron microscopy; ER, endoplasmic reticulum; LD, lipid droplet; OCR, oxygen consumption rate; Plin1, perilipin 1, perilipin A; Plin2, perilipin 2, ADFP; Plin5, perilipin 5, Lipid Storage Droplet Protein 5; PPARα, peroxisome proliferator-activated receptor α; RNAi, RNA interference; TIP47, tail interacting protein.

[1] To whom correspondence should be addressed.
e-mail: csztalry@grecc.umaryland.edu

[S] The online version of this article (available at http://www.jlr.org) contains supplementary data in the form of four figures, one table, and two videos.

associated with cellular apoptosis and heart failure (2, 3). A better understanding of the relationship between LDs and mitochondria will provide novel targets for intervention and prevention of cellular lipotoxicity, a recognized element in the pathology of numerous metabolic diseases.

RNA interference (RNAi) functional screens in *Drosophila* and mammalian cells have identified several biochemical pathways regulating LD biogenesis and utilization (4, 5). These studies established that the LD compartment is not just a passive sink storing intracellular FAs, but rather, it is a highly regulated, metabolically active organelle with a wide range of functions involving lipid flux, protein trafficking, and interaction with other organelles, including mitochondria (4–6). Emerging evidence suggests LDs and mitochondria are intimately and functionally related. Cells from oxidative tissues have high and fluctuating energy demands and exposure to FA that require efficient coupling between energy storage in LDs and utilization in mitochondria (7, 8). Mitochondrial dysfunction results in prominent lipid accumulation and tissue-specific metabolic disturbances in both mice and humans (6). Conversely, lack of some LD-associated proteins has been associated with increased mitochondrial FA β-oxidation in adipose cells (9, 10). New studies are revealing an emerging relationship between LD hydrolysis and levels of PPARα expression, an important transcription factor for mitochondrial function (11). In addition to functional interactions, spatial interaction between these two organelles has been suggested in electron microscopic (EM) studies of adipocytes, heart, and liver (12–14). In slow-twitch skeletal muscle cells where lipids are used for energy, interaction between LDs and mitochondria is enhanced by exercise training (15). Although functional and physical interactions between these two essential components of cellular energy homeostasis are well accepted, the genes and mechanisms regulating this pathway have not been identified.

LD proteomic studies identified a proteome "signature" for LDs that consistently includes at least one member of the perilipin protein family (16, 17). A perilipin protein is always present at the surface of LDs, suggesting an important structural and/or regulatory role for this class of proteins in lipid droplet formation and function. One property common to members of the perilipin protein family is their ability to act as scaffolding proteins (18, 19); however, it has yet to be established if they play an essential role in tethering LDs to organelles.

In these studies, we investigate whether perilipin proteins play a role in the physical association between LDs and mitochondria. We found that among the perilipin proteins studied, perilipin 5 (Plin5; also known as LSDP5) is uniquely associated with mitochondria in oxidative cells and tissues, especially heart, and that Plin5 has the distinctive property of recruiting mitochondria at the LD surface. We have identified a distinctive Plin5 protein domain necessary to support this function, positioned in the C terminal of the protein between amino acids (AA)343 and AA463. By inhibiting hydrolysis and stabilizing the lipid droplet, Plin5 helps to accumulate palmitate into triglycerides and to decrease palmitate utilization by the mitochondria in basal state. In protein kinase A-stimulated state, LD hydrolysis inhibition is lifted and FAs are released from LDs to undergo β-oxidation in mitochondria. These results support our hypothesis of a physical and metabolic link between LDs and mitochondria, and further, they suggest that Plin5 regulates LD hydrolysis and controls local FA flux to protect mitochondria against an FA surge. By analogy to adipose perilipin 1 (Plin1; also known as perilipin A), our studies suggest that Plin5 also plays an important role in regulating LD hydrolysis in oxidative mammalian tissues and thus is a putative key player in lipid-droplet function in oxidative tissues.

MATERIALS AND METHODS

Animals

All procedures that involved animal handling were approved by the Institutional Animal Care and Use Committee at the University of Maryland School of Medicine. The mice and rats were housed in a 12 h light/dark cycle and temperature-controlled room with access to water and food ad libitum. Mice were were fasted for 12 h (overnight) and euthanized by 6 AM; rats were fasted for 36 h and euthanized by 9 AM. Mice were male C57BL/6J (8 weeks of age); rats were male Wistar (8 weeks of age) or rat pups (postnatal day 1).

Cell culture

Primary rat neonatal cardiac myocytes, which were obtained as previously published, were cultured for 4-6 days on coverslips set in 6-multiwell dishes (20, 21). AML12 cells were obtained from ATCC (Manassas, VA) and grown according to the standard protocol. Chinese hamster ovary (CHO)-K1 and CHO Flp-In cells were purchased from ATCC and Invitrogen (Carlsbad, CA), respectively, and were grown as previously described (22). HL-1 cells were handled as previously described (22). Briefly, all confocal dishes were precoated with gelatin-fibronectin and maintained in Claycomb^{TM} medium from SFAC Biosciences (Lenexa, KS) supplemented with 10% fetal bovine serum, 2 mM L-glutamine, penicillin-streptomycin (100 μg/ml:10 μg/ml) from Invitrogen), and 0.1 mM norepinephrine from Sigma-Aldrich (St. Louis, MO). Medium was changed every 24 h. HeLa cells were grown and maintained as recommended by ATCC.

The constructs for perilipin 2-YFP (Plin2-YFP) and perilipin 5-YFP (Plin5-YFP) were introduced into the CHO Flp-In cells according to the manufacturer's instructions and were previously described (23). Stably transfected CHO Flp-In cells were selected 24 h after transfection by adding hygromycin (500 μg/ml) to the growth medium. Wild-type CHO Flp-In cells were grown in the presence of zeocin (100 μg/ml).

For immunofluorescence studies, AML12, HL-1, and CHO-K1 were seeded in 35 mm dishes with glass bottoms (MatTek Corporation, Ashland, MA) at a density of 2×10^5 cells. The following day, cells were transfected with 1 μg of DNA plasmid containing cDNA coding for the fusion protein of interest per well (cotransfection received 0.5 μg of each DNA per well) using Lipofectamine plus reagent (Invitrogen) according to the manufacturer's instructions. Four hours after transfection, cells were incubated in growth medium supplemented with 400 μM oleic acid complex to BSA overnight as described previously (24). Confocal imaging of live cells was performed at 37°C and 5% CO_2 using a Zeiss LSM510 microscope equipped with an S-M incubator (Carl Zeiss MicroImaging, Inc.) that was controlled by the CTI temperature

regulator, along with humidification and an objective heater. Emitted light was passed through band-pass filters for collection of CFP (470-510 nm), YFP (530-550 nm), and Rhodamine (541-551 nm). Seventy-two hours after plating, neonatal cardiac myocytes grown on coverslips were incubated overnight in growth medium supplemented with 400 μM oleic acid complexed to BSA, fixated with 4% paraformaldehyde in PBS, and prepared for microscopy. Fixed cells were probed with polyclonal antibodies as indicated in the figure legends. MitoTracker Red CMXRos (Invitrogen) or pECFP-mito (Clontech, Mountain View, CA) was used to label mitochondria as indicated in the figure legends.

Molecular cloning

To generate YFP fusion vectors, cDNAs of interest, wild-type Plin5, C-terminal truncated forms of Plin5, wild-type Plin2, and Plin1 were cloned in frame with monomeric pEYFP-C1 (24). Names and sequences of subcloning oligonucleotide primers for all fluorescent fusion protein constructs are presented in the supplementary Table I. As pEYFP-Plin2 and pEYFP-Plin5 are in the same pEYFP-C1 vector backbone, an In-fusion cloning kit from Clontech was used to generate a Plin2/Plin5 chimeric protein. Briefly, a PCR fragment containing Plin5 C terminal and a fragment of the vector was obtained from the pEYFP-Plin5 template using the following primer pairs: forward 5′ATGGATTACTTTGTTAACAACACGCC TCTCAA CTGGCTGGTAGGTCCCTTTTATCCTATCCTGGTGGAACAGTCGGAG-3′; reverse 5′-TGCAATAAACAAGTTAACAACAACAATTGC-3′. This PCR fragment was subcloned into pEYFP-Plin2 whose C-terminal sequence and an equivalent fragment of the vector was deleted with HpaI digestion. The resulting chimera construct encodes AA1-405 of Plin2 at the N terminus and AA396-463 of Plin5 at the C terminus. The DNA region covering the insert and chimera junction was fully sequenced to verify that no PCR-introduced mutation was present. All constructs were verified by sequencing analysis.

Adenovirus

To generate adenovirus to drive the expression of Plin5, the Plin5-YFP cDNA fragment was excised from Plin5-YFP with Xho I and Kpn I (see supplementary Table I) and was subcloned into a modified pAdTrack-CMV shuttle vector (24) lacking the GFP cassette. The PmeI-digested vector was used for transformation into AdEasy BJ5183 cells. Correct recombination of the resulting viral vector was confirmed by restriction enzyme digestion. Finally, the PacI-digested viral DNA was transfected into human embryonic kidney 293 cells for virus production and amplification (25).

Tissue processing for EM and micrograph analysis

For electron microscopy (EM), hearts were excised, quickly cut into small pieces, and fixed in-situ with Trump's fixative and postfixed in 1% osmium tetroxide (26). The same fixative was used for AML12 cells transduced with GFP-empty vector adenovirus or with Plin5-YFP adenovirus. Tissues and cells were then dehydrated in graded alcohols, en-bloc stained with uranyl acetate, and embedded in epoxy resin. One micron sections and ultrathin sections were cut on either a Porter-Bloom or LKB ultramicrotome, stained with lead acetate, and examined with either a JEOL 1200 EX or aTecnai G2. Thirty-five (heart) and 10 (AML12) fields containing longitudinally arrayed myofibrils were photographed from each section at 3,200× or 5,000× magnification. The LD number and number of LDs in close association of mitochondria were counted in each field.

Isolation of cardiac myocyte mitochondria and immunoblot analysis

Cardiac mitochondria from 8-week-old male Wistar rats fed or fasted for 36 h were isolated using methods previously described (27, 28). Briefly, freshly isolated adult cardiac myocytes were suspended in hypotonic buffer containing 250 mM sucrose, 10 mM Hepes, and 1 mM CaCl2 for 30 min to rupture the sarcolemma and release mitochondria. Cardiac myocytes were then spun at 500 *g* for 10 min at 4°C, and the supernatant containing the mitochondria was collected. The mitochondria fraction was then pelleted at 8,500 *g* for 10 min at 4°C. Following three washes and centrifugation cycles with buffer containing 150 mM KCl, 10 mM Hepes, and 1 mM $CaCl_2$ (pH 7.2) supplemented with protease inhibitors, the mitochondria pellet was resuspended in the same buffer. Ten micrograms of mitochondrial protein extracts from isolated rat cardiac myocytes was separated on 4-12% polyacylamide NuPage gels (Invitrogen), transferred to nitrocellulose membranes, probed with specific antibodies for Plin2, Plin3, Plin5, and then by a corresponding horseradish peroxidase-conjugated secondary antibody. The immunoblot signals were detected with Supersignal chemiluminescence reagents (Pierce, Rockford, IL). ATP synthase α staining and calnexin were used, respectively, as mitochondria and endoplasmic reticulum (ER) markers. Immunoblots of rat whole heart were used to check the specificity of the Plin2, Plin3, and Plin5 antibodies.

Cellular lipolysis

Lipolysis was performed as described previously (23, 24). Briefly, AML12 cells were seeded into a 24-well plate at a density of 1×10^5 cells per well, and then transduced with adenovirus driving Plin5-YFP and GFP, respectively. After 48 h, cells were incubated overnight with growth medium supplemented with 400 μM oleic acid complexed to 0.4% BSA to promote triacylglycerol deposition. [^{3}H]Oleic acid, at 2×10^6 dpm/well, was included as a tracer. Supplemental fatty acids were then removed and reesterification of fatty acids during subsequent incubations was prevented by inclusion of 5 μM Triacsin C (Biomol, Plymouth Meeting, PA), an inhibitor of acyl coenzyme A synthetase, in the medium. Some cells were also supplemented with etomoxir (Sigma-Aldrich), an irreversible *O*-carnitine palmitoyltransferase-1 (CPT-1) inhibitor, to inhibit β-oxidation during lipolysis. Quadruplicate wells were tested for each condition. Lipolysis was determined by measuring radioactivity released in media (23). Efficiency of transduction with Ad-Plin5-YFP was checked by immunoblotting.

β-oxidation measurements

Assessment of the effects of ectopic Plin5 protein on fatty acid β-oxidation was performed using respirometry measurements (29) and metabolic radioactive labeling (30). To control for cell number seeding concentration, AML12 cells were first transduced with adenovirus driving the expression of GFP alone (control) or Plin5-YFP, then trypsinized 48 h following infection, and reseeded in XF24 V7 24-well microplates (Seahorse Bioscience, North Billerica, MA) at 4×10^4 cells in each well. Cell respiration was assayed using a high-throughput respirometer (Seahorse Bioscience) to perform time-resolved measurements of oxygen consumption rate (OCR). Fatty acid β-oxidation was measured as described by the manufacturer by sequentially injecting 200 μM palmitate conjugated with BSA (1:6) and 50 μm etomoxir in buffered KHB (110 mM NaCl, 4.7 mmol/l KCl, 2 mmol/l $MgSO_4$, 1.2 mmol/l Na2HPO_4, 2.5 mmol/l glucose adjusted to pH7.4) supplemented with 50 μm carnitine. β-oxidation using metabolic radioactive labeling was performed in control or Plin5-YFP cells as described (30). Cells were seeded in a 24-multiwell dish and exposed to DMEM supplemented with 0.24 mmol/l fatty acid-free albumin (BSA), 0.5 mmol/l L-carnitine, 20 mmol/l HEPES, and [1-^{14}C] palmitate (1.0 μCi/ml, 0.017 mmol/l) with 5 mmol/l glucose (30). After CO_2 trapping, the incubation media were transferred to new tubes and assayed for labeled β-oxidation

products (acid-soluble metabolites [ASM]) (30). The protein content of each sample was determined as described previously (23). Pulse chase experiments were performed according to ref. 31 with some modifications. AML12 cells were infected with adenovirus for 24 h and incubated with 1 μCi [1-^{14}C]oleate in the presence of 400 μM unlabeled oleate, which was used to avoid lipotoxicity. After an overnight incubation, cells were washed twice with 1% BSA in PBS and then incubated for an additional 6 h in MEM media with 1 mM carnititne without added oleate (chase) in the presence or not of 20 μM of forskolin. CO_2 trapping was performed as above.

Incorporation of [^{14}C] palmitate into triglyceride and phospholipids

AML12 cells transduced with adenovirus driving the expression of GFP alone or Plin5-YFP were seeded in a 24-well plate. Cells were incubated in growth medium supplemented with 200 μM palmitate conjugated with BSA (6:1) including 0.2 μCi of [^{14}C] palmitate for 6 h (30). Lipids were extracted by the Bligh-Dyer method (32) and analyzed by thin layer chromatography by using chloroform/acetone/acetic acid (96:4:1) as described (33). Incorporation of [^{14}C] palmitate into triglyceride and phospholipids was normalized for protein concentration.

Statistical analysis

Statistical significance was tested using either one-way ANOVA or two-tailed Student *t*-test (GraphPad Software).

RESULTS

Perilipin 5 recruits mitochondria at the LD surface

A histological examination of tissues from left ventricle muscle from mice by transmission electronic microscopy showed that fasting results in increased LD size and number (average diameter of LDs in fed = 0.49 ± 0.03 μm versus fasted = 1.34 ± 0.05 μm, $P < 0.01$; LDs counted in fed = 70 versus fasted = 209, $P < 0.01$). Importantly, 90% of LDs were located within clusters of mitochondria between the fibrils with fasting (**Fig. 1A**) (34). The expression profile of perilipin proteins was assessed by Western blot. As reported before, Plin5 and perilipin 2 [Plin2; also known as adipose differentiation-related protein (ADFP)] protein expression levels in mice heart extracts were found to be regulated with fasting, whereas Plin3 was not (Fig. 1B) (35). Plin4 was undetected using a commercially available antibody (results not show). Because of difficulty in obtaining isolated lipid droplets from heart tissue, the subcellular distribution of mitochondria and LDs was investigated in neonatal cardiac myocytes, a cell culture model that expresses detectable levels of endogenous Plin5 at the LD surface in response to fatty acid incubation (**Fig. 2**). Plin2 and Plin3 at the LD surface were also detected in these cells, but Plin1 and Plin4 were undetectable (data not shown). In neonatal cardiac myocytes, LDs appeared as individualized units in response to FA load (**Figs. 2, 3**) and were not organized in clusters, as has been observed in CHO-K1 or AML12 cell lines (36, 37), (**Figs. 4, 5**). α-Actinin, the major Z-disk protein, was used as a marker for cardiac myocytes. All cells examined by confocal microscopy that stained positively for Plin5 were also positive for α-actinin immunostaining. Interestingly, mitochondria

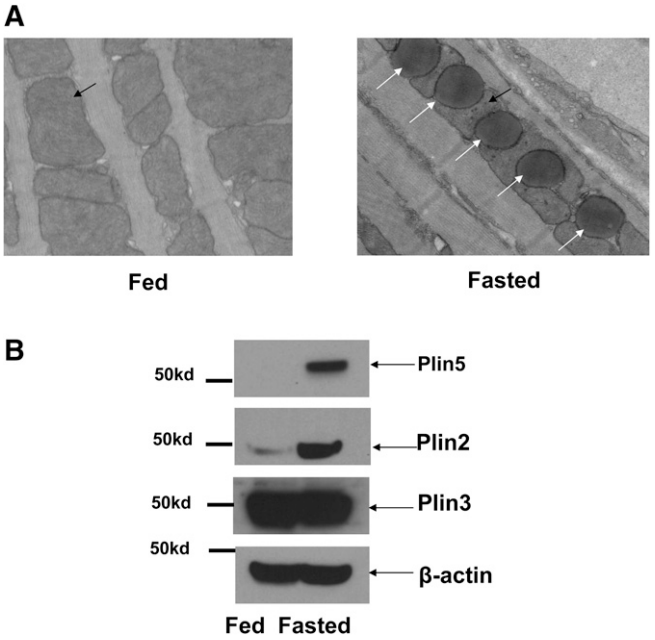

Fig. 1. Lipid droplet accumulation in the heart is a physiological adaptation to fasting. (A) Left heart ventricles from fed and 24 h fasted mice were excised in the indicated conditions and fixed with Trump's fixative, postfixed in 1% osmium tetroxide. Thin sections were stained with lead citrate and uranyl acetate and investigated with transmission EM. Two mice per group and six positions per sample were randomly investigated, and representative photographs are presented. Black arrows indicate mitochondria, and white arrows indicate lipid droplets. Magnification: 5000×. (B) Perilipin protein expression from mice heart in fed and fasted conditions by Western blot (WB) using Plin2, Plin3, and Plin5 antibodies. β-actin antibody was used as a loading control.

were localized around LDs as revealed by costaining the cells with Plin5 and MitoTracker, a commercially available mitochondria dye (Fig. 3A).

Although it is well established that all perilipin proteins associate with LDs (19, 20), it is not clear whether they are found in mitochondria. Therefore, we assessed the association of perilipin proteins with the mitochondrial fraction isolated from adult rat hearts. Because rats are larger rodents, rat hearts are easier to perfuse to obtain cardiomyocytes and proceed with the isolation of the mitochondria fraction. In fasted rats, freshly isolated mitochondria were found to be enriched in Plin5, but not in Plin2 or Plin3, as determined by Western blot (Fig. 3B). As a positive control, we fractionated whole-cell lysates by SDS-PAGE, followed by Western blotting to confirm the presence of all three perilipin proteins in the adult rat heart (Fig. 3B). Purity of the mitochondrial fraction was tested on immunoblots using anti-calnexin, an ER marker, and anti-ATPase α antibodies. Perhaps due to differences in timing of feeding and euthanasia between mice and rats, Plin5 and Plin2 protein expressions from rat whole heart did not appear to be strongly affected by nutritional status (Fig. 3B), contrary to the mouse model (Fig. 1B).

To further explore whether the LD coat protein composition could affect cellular mitochondria distribution, we used CHO cell lines stably expressing fluorescent protein

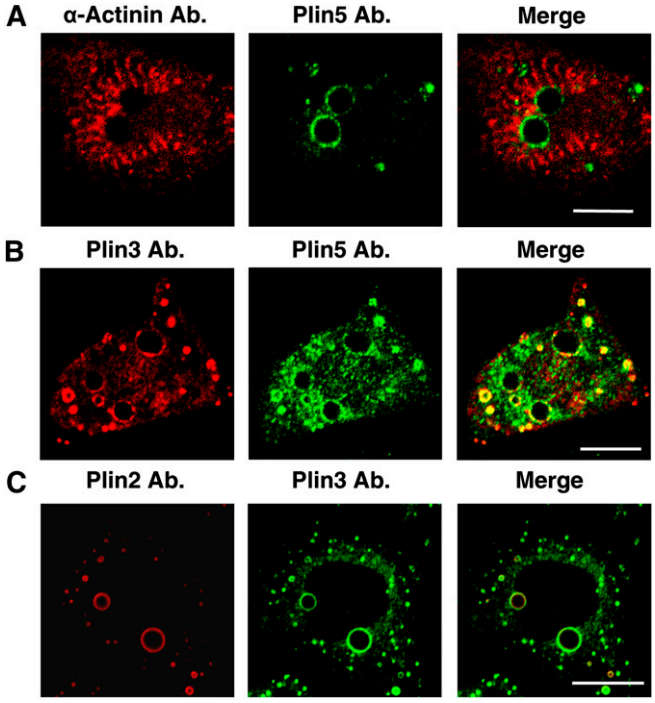

Fig. 2. Presence of Plin5, Plin3, and Plin2 at the surface of LDs of neonatal rat cardiac myocytes. Neonatal rat cardiac myocytes from fed and fasted rats were incubated overnight with 400 μM oleic acid before fixing cells with paraformaldehyde. Cells were costained with antibodies against (A) α-myosin and Plin5, (B) Plin3 and Plin5, and (C) Plin2 and Plin3, and confocal microscope images obtained. Merged images show coincident staining in yellow. Micrographs depict one or two representative cells of hundreds observed in three experiments. Bar: 10 μm.

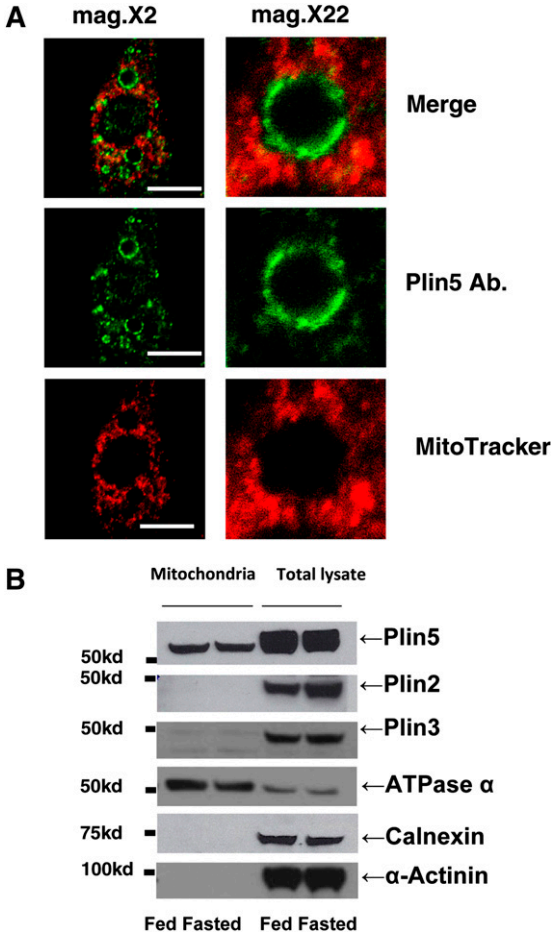

Fig. 3. Close proximity between LDs and mitochondria in neonatal cardiac myocytes and Plin5 is uniquely associated with freshly isolated mitochondria from rat left heart ventricle heart. (A) Neonatal rat cardiac myocytes were incubated overnight with 400 μM oleic acid before being stained with MitoTracker (1 μM) for 30 min. and fixed with 3% paraformaldehyde. Cells were stained with antibody against Plin5, and confocal microscopy was performed as in Fig. 1. Bar: 10 μm. Magnification: 2× and 16×. Micrographs show one representative cell of hundreds observed in three experiments. (B) Perilipin protein expression in heart mitochondria fractions isolated by differential centrifugation or whole-cell extracts in rat fasted for 36 h. Each lane contains equal amounts of mitochondria protein extract from heart (10 μg) or whole-protein extract (100 μg) for Plin 2, Plin3, Plin5, calnexin, and α-actinin and whole protein-extract (30 μg) for ATPase α from rat heart. One representative experiment is shown.

fusion constructs for Plin1, Plin2, and Plin5 with MitoTracker to allow live cell imaging. Observations by confocal microscopy revealed important differences. In the cytoplasm of cells expressing Plin1 and Plin2, mitochondria were distributed at the periphery of existing LD clusters. In contrast, the mitochondria of cells expressing Plin5 were observed to be almost exclusively localized within LD clusters (Fig. 4). Transient expression of Plin5-YFP induced a similar distribution pattern of mitochondria in representative oxidative tissue cell lines, such as liver AML12 cells and cardiac muscle HL-1 cells (Fig. 5A). The cellular organelle reorganization was limited to the mitochondria and did not result in obvious ER pattern alteration (supplementary Fig. I). We confirmed that a similar pattern of mitochondria distribution was observed in AML12 cells expressing his-tagged Plin5, a smaller tag peptide than the YFP protein (supplementary Fig. II-A). By coexpressing cytochrome C-CFP and Plin5 in AML12 cells, we also confirmed that the use of MitoTracker was not responsible for the mitochondria/Plin5-coated LD interaction (supplementary Fig. II-B). Treatment with etomoxir (an inhibitor of mitochondrial carnitine palmitoyltransferase-1) or FCCP (an uncoupler agent) did not alter the association between Plin5-coated LDs and mitochondria (results not shown). Finally, EM revealed a physical association between LDs and mitochondria in AML12 cells transduced with adenovirus expressing Plin5-YFP (Fig. 5B and supplementary Fig. III). All LDs examined were associated with at least one mitochondria. Interestingly, mitochondria in close physical interaction with Plin5-coated LDs do not appear to have the same motility and dynamic as do mitochondria in cells with Plin2-coated LDs (supplementary videos I and II). We next investigated whether this physical link was due to a specific peptide sequence in Plin5.

The last 20 amino acids of the C terminus of perilipin 5 are responsible for the physical interaction observed between LDs and mitochondria

To further identify the sequence of Plin5 that allows LDs to physically interact with mitochondria, two truncated C-terminal fluorescent Plin5-YFP fusion proteins,

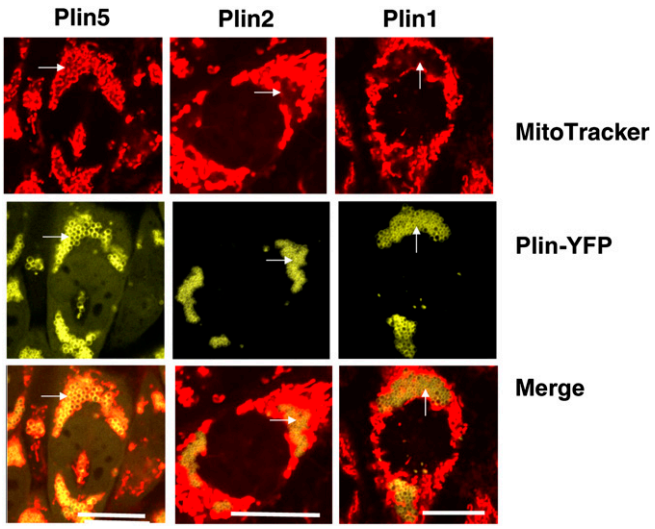

Fig. 4. Mitochondria are uniquely associated to Plin5-coated LDs in CHO-K1 cells. CHO-Flp-In cells constitutively expressing Plin5-YFP, Plin1-YFP, and Plin2-YFP were incubated with 400 μM oleic acid overnight. The following day, cells were incubated with MitoTracker (1 μM) for 30 min, and confocal microscopy was performed as in Fig. 1. Micrographs depict one or two representative cells of hundreds observed in three experiments. Bar: 10 μm. White arrows indicate LDs.

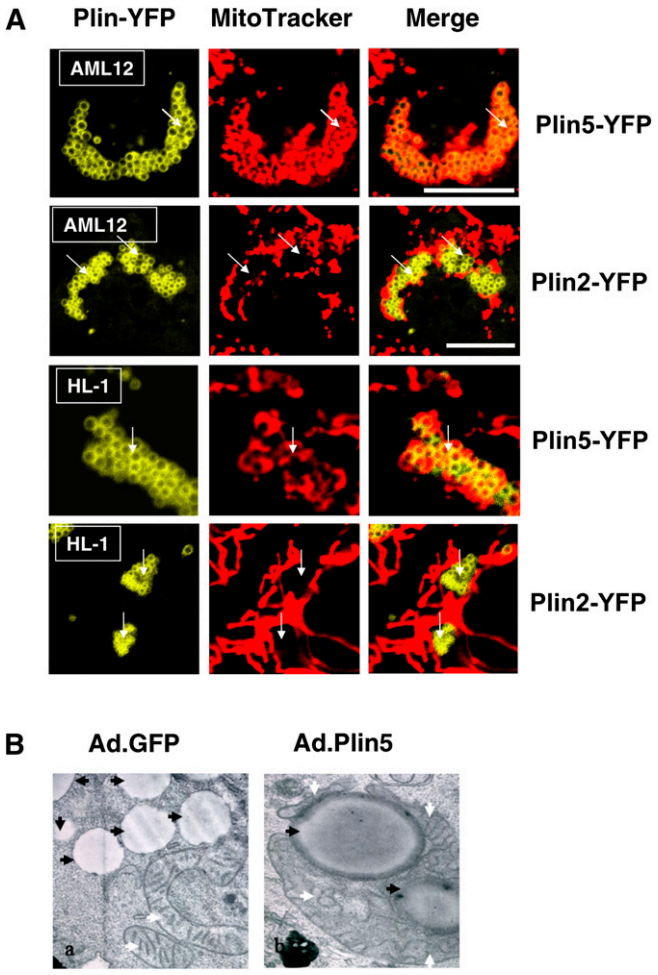

Fig. 5. Plin5 recruits mitochondria in a cell type-independent manner. (A) Murine AML12 cells (liver; top row) and HL1 cells (heart; bottom row) were transfected with Plin5-YFP or Plin2-YFP and incubated with 400 μM oleic acid overnight. The following day, cells were incubated with MitoTracker (1 μM) for 30 min, and confocal microscopy was performed as in Fig. 1. Micrographs show merged image obtained for Plin-YFP and MitoTracker in representative cells from two to three separate experiments. Bar: 10 μm. White arrows indicate LDs. (B) AML12 (liver) cells were transduced with GFP-adenovirus or Plin 5-YFP adenovirus and TEM was performed. White arrows indicate mitochondria, black arrows indicate LD. Magnification: 10,000×.

AA1-391 and AA1-188, were expressed in AML12 cells and stained with MitoTracker. As shown in **Fig. 6**, both full-length (wild-type) and truncated C-terminal Plin5 proteins targeted LDs; however, the association between LDs and mitochondria was only observed when wild-type Plin5 was expressed. Even more compelling evidence for a specific function within the C terminal of Plin5 was provided by a chimera constructed of both Plin2 and Plin5 (Plin2/Plin5). The chimeric design utilized the N terminus of Plin2 fused to the C terminus of Plin5 [N-Plin2 (AA1-AA405)/C-Plin5 (AA306-AA463)]. LDs with a surface coated with the N-Plin2/C-Plin5 chimera were able to bind and recruit mitochondria (**Fig. 7A**), whereas wild-type Plin2 could not recruit mitochondria at the LD surface (Fig. 7B), as expected (see Fig. 5A). Absence of the last 20 AA of the C terminus of the chimera was sufficient to inhibit mitochondrial clustering around LDs; thus, this peptide is a necessary sequence for interaction between these two organelles (Fig. 5C). Sequence analysis revealed this Plin5 domain to be highly conserved among species (Fig. 7D).

Perilipin 5 stabilizes LDs by inhibiting LD hydrolysis and helps to channel saturated palmitic acid into triglyceride and decrease palmitic acid utilization by the mitochondria

We confirmed our previous report that Plin5 prevented LD hydrolysis in liver AML12 cells (**Fig. 8A**) in basal conditions (24). Pharmacological inhibition of mitochondrial carnitine palmitoyltransferase-1 with etomoxir did not affect the amount of radioactive FA released by control cells or cells overexpressing Plin5 (Fig. 8A). Triacsin C, a pharmacological inhibitor of fatty acyl-CoA synthetase, efficiently suppressed FA acylation and β-oxidation in this cell system under these experimental conditions (23). To test whether Plin5 stabilization of LDs reflects channeling of exogenous palmitate to triglyceride stores and away from the mitochondria utilization pathway, we performed metabolic radioactive palmitate labeling (Figs. 8B) and respirometry measurements (Fig. 8C). While cells expressing GFP and Plin5 incorporated more palmitate into their triglyceride fraction than into their phospholipid fraction, cells overexpressing Plin5 incorporated significantly more palmitate into their triglyceride fraction (Fig. 8B). Presence of Plin5 at the LD surface did not affect the incorporation of palmitate into the phospholipid fraction (Fig. 8B). Oxidation of exogenous FA can be assessed by monitoring cellular oxygen consumption upon addition of an FA, such as palmitate, using the Seahorse technology. We observed an increased OCR in AML12-cultured cells transduced with adenovirus GFP or Plin5-YFP cells in medium upon addition

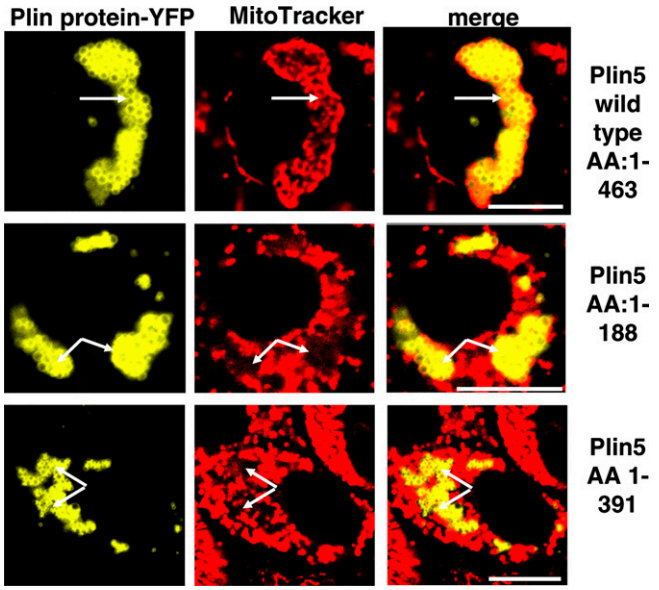

Fig. 6. Perilipin 5 domain between AA 391and AA 463 is responsible for mitochondria recruitment. Plasmids for fusion constructs of wild-type Plin5, Plin5 (AA1-AA188), and Plin5 (AA 1-AA391) with YFP were transfected in CHO-K1 cells and incubated with 400 μM oleic acid overnight. The following day, cells were incubated with MitoTracker (1 μM) for 30 min, and confocal microscopy was performed as in Fig. 1. Bar: 10 μm. White arrows indicate lipid droplets. Top, middle, and bottom rows show representative cells from two to three separate experiments.

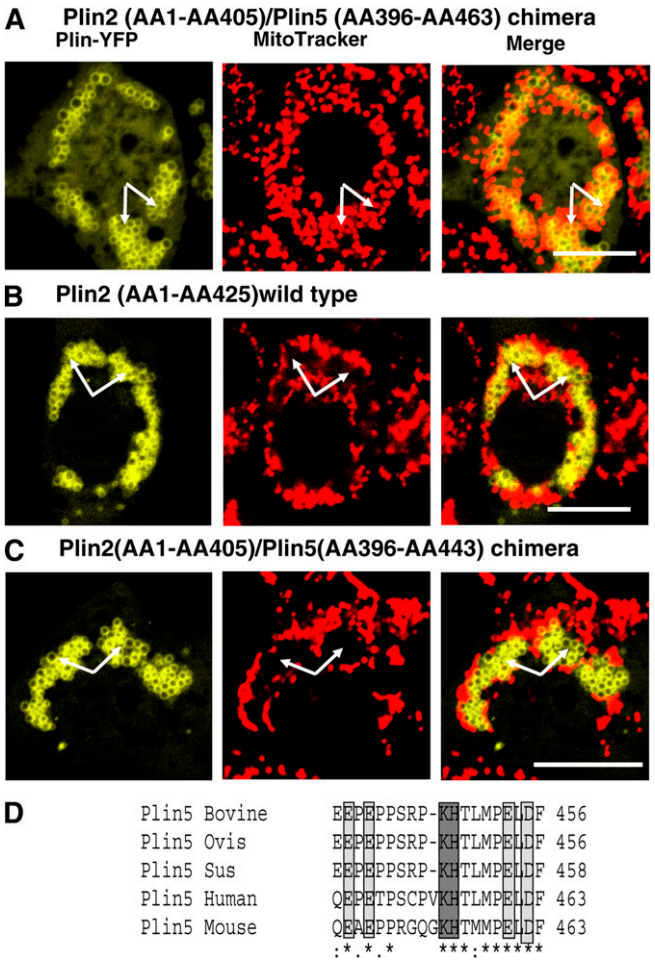

Fig. 7. The Plin5 C-terminal domain is necessary to recruit mitochondria. Plasmids for fusion constructs of (A) chimera protein Plin2 (AA1-AA405)/Plin5 (AA396-AA463), (B) wild-type Plin2, and (C) chimera protein Plin2 (AA1-AA405)/Plin5 (AA396-AA443) with YFP were transfected in CHO-K1 cells and incubated with 400 μM oleic acid overnight. The following day, cells were incubated with MitoTracker (1 μM) for 30 min, and confocal microscopy was performed as in Fig. 1. Bar: 10 μm. White arrows indicate LDs. Top, middle, and bottom rows show representative cells from two to three separate experiments. (D) A schematic view for Plin5 C-terminal domain and protein sequence similarity among species. Positive charge polar AA (dark gray) and negative charge polar AA (light gray) are highlighted.

of palmitate, which was subsequently blunted by etomoxir (results not shown), suggesting that AML12 cells can take up and oxidize exogenous FA. However, the presence of Plin5 blunted the induction of O_2 consumption by palmitate, which was confirmed by determining the contribution of lipid oxidation to total O_2 consumption by blocking mitochondrial FA uptake with etomoxir (Fig. 8C, part a). These differences were observed in the absence of a significant difference in amount of ATP synthase α present in cells with or without Plin5 expression as determined by Western blot (Fig. 8C, part b). Complementary experiments using radiolabeling techniques confirmed these findings. Overexpression of Plin5 resulted in a 28% and 23% decrease in CO_2 and ASM production, respectively, when cells were pulsed with 100 μM [1-^{14}C] palmitate. [Values for CO_2 are expressed in dpm/mg protein ad.GFP (9,017 ± 1,001) versus ad.Plin5 (6,534 ± 378), $P < 0.05$. Values for ASM are expressed in dpm FA/mg protein ad. GFP (28,834 ± 760) versus ad.Plin5 (22,102 ± 686), $P < 0.05$.] We recently reported that Plin5-like adipose tissue Plin1 is a protein kinase A-phosphorylated protein and that cells overexpressing Plin5 have increased lipolysis following forskolin incubation (24). We performed pulse chase experiments to measure the contribution of LD hydrolysis to provide FA substrate to the mitochondria in presence or absence of forskolin during the chase. Overexpression of Plin5 resulted in a 54% decrease in CO_2 when cells were pulsed with 400 μM [1-^{14}C]oleate and chased for 6 h in basal conditions, but differences were no longer observed when cells were chased in the presence of forskolin. [Values for CO_2 from four separate experiments are expressed in dpm/mg protein in the absence of forskolin ad.GFP (32,394 ± 4,250) versus ad.Plin5 (17,606 ± 1,692), $P < 0.05$. In the presence of forskolin, ad.GFP (34,535 ± 2,964) versus ad.Plin5 (26,600 ± 1738), not significant.]

DISCUSSION

A major finding of this study is that Plin5 induces physical contact between LD and mitochondria. In addition, at the metabolic level, we show that Plin5 stabilizes LDs by inhibiting hydrolysis and channeling FAs to triglyceride stores at the expense of FA oxidation by the mitochondria, and Plin5 releases FA to mitochondria β-oxidation when adenyl cyclase is activated with forskolin. Together these

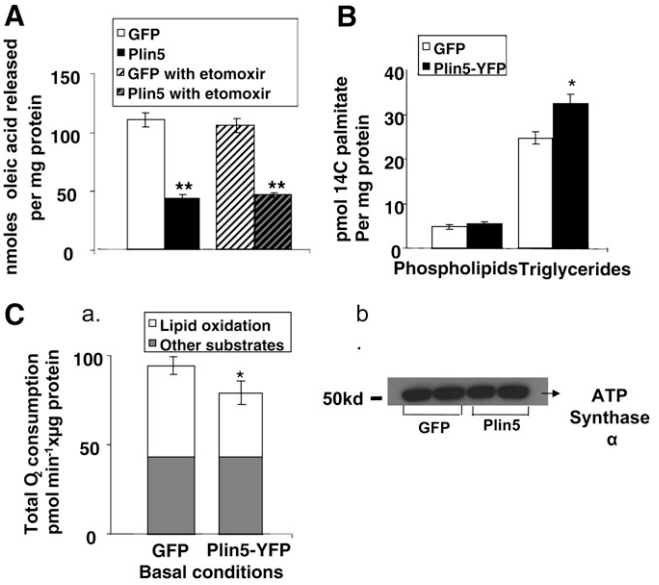

Fig. 8. Plin5 effect on lipolysis, palmitate incorporation in cellular phospholipids, and triglyceride and palmitate β-oxidation. (A) AML12 cells were transduced with an adenoviral construct for the expression of GFP or Plin5 constructs for 48 h prior to lipolysis measurements. Cells were loaded overnight with [^{3}H]oleic acid and 400 μM unlabeled oleic acid. Supplemental fatty acids were removed and 5 μM triacsin C with or without etomoxir (50 μM) was added to the medium for 2 h. Release of fatty acids is shown. Data represent means ± SEM (n = 16). ** $P < 0.01$ for cells expressing GFP compared with cells expressing Plin5. (B) AML12 cells were transduced with an adenoviral construct for the expression of GFP or Plin5 constructs for 48 h. Cells were supplemented with media containing 200 μM palmitate in the presence of 0.2 μCi of [^{14}C]palmitate. Incorporation of [^{14}C]palmitate into triglyceride and phospholipids was measured after 6 h. Bar graph displays palmitate incorporation per micrograms of cellular protein in phospholipid and triglyceride fraction separated by thin layer chromatography. Data are the average ± SEM for two samples from four independent experiments. (C) (a) AML12 cells were transduced with an adenoviral construct for the expression of GFP or Plin5 constructs for 48 h prior to lipolysis measurements. Cells were replated in Seahorse 24 multiwells. After being equilibrated for 2 h in assay buffer, each well was sequentially injected with palmitic acid (200 μM) and etomoxir (50 μM). Total length of the bar equals total O_2 consumption. Gray part of the bar is the O_2 consumption in each group when treated with etomoxir. Therefore, the white part represents lipid oxidation-derived O_2 consumption. Data is represented as oxygen consumption above baseline and normalized to cellular proteins ± SEM (triplicate wells, n = 3 separate experiments). *Statistical difference versus respective control adenoviral GFP at $P < 0.05$. (b) Western blots indicating levels of ATP synthase α in representative wells collected at the end of the experiment.

findings suggest that Plin5 plays an important role in oxidative tissues by decreasing the exposure of mitochondria to FA by storing FA transiently in the LD compartment as neutral triglyceride and by regulating LD hydrolysis, thus acting to protect mitochondria from a local surge in FA flux.

We show that Plin5 has the unique property of recruiting mitochondria at the LD surface with the binding site on the C terminal 20AA of the Plin5 sequence. These AA residues appear to be highly conserved among Plin5 proteins, but they are not shared with other perilipin family members. This targeting signal is necessary to induce physical contact between mitochondria at the LD surface. Mitochondria protein import and recognition is generally directed by an N-terminal or, less frequently, by a C-terminal signal sequence consisting of ~20-30 amino acid residues (36). Comparisons of known sequences have revealed that they do not share a common primary structure (36). In these cases, however, a common secondary structure, as well as certain basic, hydrophobic and polar residues, might be present (36). The conserved Plin5 mitochondria-targeting domain contains hydrophilic and ionic (D, E, K, H) amino acids and is enriched in proline. It contains two polar positively charged residues, histidine and lysine. However, introducing single point mutations [H to alanine (A) and K to A] did not affect the ability of Plin5 to recruit to mitochondria (results not shown). Therefore, additional work will be required to investigate how this C-terminal Plin5 peptide elicits such an activity.

Members of the perilipin protein family share a high primary sequence homology, especially at the N terminal (20, 34). A comparison of murine Plin5 sequence with other perilipins reveals that its highest sequence similarity is to Plin2 and Plin3. Interestingly, *Plin3*, *Plin4*, and *Plin5* genes are mapped to the same chromosome in mammalian species, and *Plin5* is located adjacent to *Plin4* and in close proximity to *Plin3* (34). It was suggested that *Plin3* is most likely the primordial gene and that evolution-driven gene duplication led to *plin4* and *plin5* as orthologs. This implies that Plin3, Plin4, Plin5 proteins will share related structures but will have more specialized functions. The ability to constitutively recruit mitochondria to LDs appears to be unique to Plin5, at least in our experimental conditions. Interestingly, Plin3 was recently reported to associate to the mitochondria fraction, but this connection happened only under specific stress conditions in cell cultures and it required an intact Plin3 N-terminal domain (38), suggesting a different mechanism for Plin3 and Plin5 to associate with the mitochondria. From qualitative microscopic observations in mature rodent adipocytes, 3T3-L1 cells, and oocytes, it is clear that occasional spatial interaction between these organelles are not solely dependent of the presence of Plin5 at the LD surface, as these cell systems do not express Plin5 (39, 40). Spatial interactions between peroxisomes and LDs have also been reported in yeast, a nonmammalian model system that does not express known perilipin protein orthologs (41). Unique to the presence of Plin5 at the LD surface is the extent by which the subcellular reorganization of mitochondria occurs. By its property of recruiting mitochondria to LDs, Plin5 can be used as a convenient tool to initiate studies exploring the spatial relationships between mitochondria and LDs.

LDs and mitochondria are known to be highly dynamic organelles. Recently, ex vivo experiments revealed one soluble N-ethylmaleimide sensitive fusion proteins attachment protein receptor protein, SNAP23, to be important in recruiting mitochondria at the Plin2-coated LD surface (42). Downregulation of SNAP23 by RNAi did not inhibit the recruitment of mitochondria at the Plin5-coated LD

surface (supplementary Fig. IV). However, SNAP23 is highly expressed in AML12 cells, and it cannot be ruled out that some SNAP23 residual activity after small interfering RNA treatment may have hampered the outcome of our experiments. Clearly, further studies are needed to confirm or identify proteins involved in the spatial relationship between LDs and mitochondria.

Even more intriguing is the need to establish a functional relevance of spatial relationships between Plin5-coated LDs and mitochondria. Among the perilipin proteins, Plin1 is the most studied, but little is known about Plin5 (20). On the basis of current knowledge, Plin5 tissue expression is limited to oxidative tissues such as heart, slow-twitch skeletal muscles, brown adipocytes, and liver. It is regulated by PPARs, suggesting an important role in FA utilization and lipid metabolism (35, 43, 44). At the cellular level, our previous work and that of others have shown that Plin5 plays an important role regulating LD accumulation (35, 43, 44) and LD hydrolysis (35). At the molecular level, it was recently reported that Plin5 is a scaffolding protein for key lipolytic players, such as adipose triglyceride lipase (ATGL) (24, 45), hormone sensitive lipase (23), and comparative gene identification-58 (24, 46). In addition, activation of adenyl cyclase by forskolin increased ^{32}P incorporation into perilipin 5 and relieved the inhibitory effect of Plin5 on lipolysis (24). Plin5 has been referred to as an exchangeable perilipin protein existing either in the cytosol in the absence of active triglyceride synthesis or in an LD-bound state when triglyceride synthesis is active (47). It is proposed that diacylglyerol content at the surface of a nascent LD surface will recruit Plin5 to the LD surface (48). Our present study indicates that Plin5, through its C terminus, may facilitate LD/mitochondria cellular reorganization, suggesting that Plin5 may play a part in protection against cellular lipotoxicity in oxidative cells with high energy demands by transiently entrapping bioactive lipids in LDs close to mitochondria at times of increased cellular FA influx and may facilitate the release of FA by LDs to the mitochondria in a PKA-regulated manner. Spatial compartmentalization of lipid synthesis and storage has already been reported. For example, Acyl-CoA:diacylglycerol acyltransferase 2 (DGAT2), a major enzyme of triglyceride synthesis, is not localized only to the ER; it is also dynamically associated with LDs and the mitochondria-associated membranes (MAM) and mitochondrial compartments, which are important during active lipid synthesis (49).

The significance of LD metabolism and, more specifically, LD hydrolysis in heart was revealed by the unexpected phenotype of the whole-body ATGL-ko mice (50). These mice exhibit massive accumulation of triglyceride in the heart, cardiomyopathy, and shortened life expectancy, which can be partially reverse by treatment with a PPARα agonist (50, 51). Patients with defective ATGL function also suffer cardiomyopathy, illustrating the importance of proper LD hydrolysis regulation in mammalian heart (52). By regulating ATGL activity and promoting physical interaction between LDs and mitochondria, Plin5 has the potential to be a key gene regulating cardiac LD hydrolysis and to play an important role in fuel delivery for mitochondria function (53).

In summary, we present the novel finding that Plin5 induces physical contact with mitochondria and regulates LD hydrolysis by channeling FA to triglyceride stores and releasing FA to mitochondrial FA oxidation. Our findings support and confirm the view that lipid storage is characterized by a reorganization of organelles to maximize this process and is cell type-specific. Further studies are necessary to fully investigate Plin5 function in oxidative tissues and to address how energy metabolism is related to physical structure in normal and lipotoxic environments.

The authors thank Dr. Martin Woodle for careful review and helpful editing of the manuscript, Dr. Orian Shirihai for helpful and lively discussion, and Mrs. Ming Bell for her technical help. The authors thank Dr. Meredith Bond for facilitating access to neonatal cardiac myocytes and Dr. Wenhong Xu for the isolation of rat cardiomyocytes and mitochondria. The authors thank Mr. Samuel Woodle for helping with computer imaging software.

REFERENCES

1. Unger, R. H., G. O. Clark, P. E. Scherer, and L. Orci. 2010. Lipid homeostasis, lipotoxicity and the metabolic syndrome. *Biochim. Biophys. Acta.* **1801:** 209–214.
2. Beller, M., C. Sztalryd, N. Southall, M. Bell, H. Jäckle, D. S. Auld, and B. Oliver. 2008. COPI complex is a regulator of lipid homeostasis. *PLoS Biol.* **6:** e292.
3. Cornier, M. A., D. Dabelea, T. L. Hernandez, R. C. Lindstrom, A. J. Steig, N. R. Stob, R. E. Van Pelt, H. Wang, and R. H. Eckel. 2008. The metabolic syndrome. *Endocr. Rev.* **29:** 777–822.
4. Mittra, S., V. S. Bansal, and P. K. Bhatnagar. 2008. From a glucocentric to a lipocentric approach towards metabolic syndrome. *Drug Discov. Today.* **13:** 211–218.
5. Guo, Y., T. C. Walther, M. Rao, N. Stuurman, G. Goshima, K. Terayama, J. S. Wong, R. D. Vale, P. Walter, and R. V. Farese. 2008. Functional genomic screen reveals genes involved in lipid-droplet formation and utilization. *Nature.* **453:** 657–661.
6. Zehmer, J. K., Y. Huang, G. Peng, J. Pu, R. G. Anderson, and P. Liu. 2009. A role for lipid droplets in inter-membrane lipid traffic. *Proteomics.* **9:** 914–921.
7. Marín-García, J., and M. J. Goldenthal. 2008. Mitochondrial centrality in heart failure. *Heart Fail. Rev.* **13:** 137–150.
8. Reichmann, H., and R. Gold. 1991. Myopathies and cardiomyopathies: histochemical and biochemical analyses. *Eur. Heart J.* **12:** 169–170.
9. Nishino, N., Y. Tamori, S. Tateya, T. Kawaguchi, T. Shibakusa, W. Mizunoya, K. Inoue, R. Kitazawa, S. Kitazawa, Y. Matsuki, et al. 2008. FSP27 contributes to efficient energy storage in murine white adipocytes by promoting the formation of unilocular lipid droplets. *J. Clin. Invest.* **118:** 2808–2821.
10. Saha, P. K., H. Kojima, J. Martinez-Botas, A. L. Sunehag, and L. Chan. 2004. Metabolic adaptations in the absence of perilipin: increased beta-oxidation and decreased hepatic glucose production associated with peripheral insulin resistance but normal glucose tolerance in perilipin-null mice. *J. Biol. Chem.* **279:** 35150–35158.
11. Sapiro, J. M., M. T. Mashek, A. S. Greenberg, and D. G. Mashek. 2009. Hepatic triacylglycerol hydrolysis regulates peroxisome proliferator-activated receptor alpha activity. *J. Lipid Res.* **50:** 1621–1629.
12. Blanchette-Mackie, E. J., and R. O. Scow. 1983. Movement of lipolytic products to mitochondria in brown adipose tissue of young rats: an electron microscope study. *J. Lipid Res.* **24:** 229–244.
13. Jacob, S. 1987. Lipid droplet accumulation in the heart during fasting. *Acta Histochem.* **82:** 149–152.
14. Vilaró, S., and M. Llobera. 1988. Uptake and metabolism of Intralipid by rat liver: an electron-microscopic study. *J. Nutr.* **118:** 932–940.

15. Tarnopolsky, M. A., C. D. Rennie, H. A. Robertshaw, S. N. Fedak-Tarnopolsky, M. C. Devries, and M. J. Hamadeh. 2007. Influence of endurance exercise training and sex on intramyocellular lipid and mitochondrial ultrastructure, substrate use, and mitochondrial enzyme activity. *Am. J. Physiol. Regul. Integr. Comp. Physiol.* **292:** R1271–R1278.
16. Liu, P., Y. Ying, Y. Zhao, D. I. Mundy, M. Zhu, and R. G. Anderson. 2004. Chinese hamster ovary K2 cell lipid droplets appear to be metabolic organelles involved in membrane traffic. *J. Biol. Chem.* **279:** 3787–3792.
17. Brasaemle, D. L., G. Dolios, L. Shapiro, and R. Wang. 2004. Proteomic analysis of proteins associated with lipid droplets of basal and lipolytically stimulated 3T3-L1 adipocytes. *J. Biol. Chem.* **279:** 46835–46842.
18. Londos, C., C. Sztalryd, J. T. Tansey, and A. R. Kimmel. 2005. Role of PAT proteins in lipid metabolism. *Biochimie.* **87:** 45–49.
19. Bickel, P. E., J. T. Tansey, and M. A. Welte. 2009. PAT proteins, an ancient family of lipid droplet proteins that regulate cellular lipid stores. *Biochim. Biophys. Acta.* **1791:** 419–440.
20. Lokuta, A., M. S. Kirby, S. T. Gaa, W. J. Lederer, and T. B. Rogers. 1994. On establishing primary cultures of neonatal rat ventricular myocytes for analysis over long periods. *J. Cardiovasc. Electrophysiol.* **5:** 50–62.
21. Russell, M. A., L. M. Lund, R. Haber, K. McKeegan, N. Cianciola, and M. Bond. 2006. The intermediate filament protein, synemin, is an AKAP in the heart. *Arch. Biochem. Biophys.* **456:** 204–215.
22. Claycomb, W. C., N. A. Lanson, Jr., B. S. Stallworth, D. B. Egeland, J. B. Delcarpio, A. Bahinski, and N. J. Izzo, Jr. 1998. HL-1 cells: a cardiac muscle cell line that contracts and retains phenotypic characteristics of the adult cardiomyocyte. *Proc. Natl. Acad. Sci. USA.* **95:** 2979–2984.
23. Wang, H., L. Hu, K. Dalen, H. Dorward, A. Marcinkiewicz, D. Russel, D. Gong, C. Londos, T. Yamaguchi, C. Holm, et al. 2009. Activation of hormone-sensitive lipase requires two steps: protein phosphorylation and binding to the PAT-1 domain of lipid droplet coat proteins. *J. Biol. Chem.* **284:** 32116–32125.
24. Wang, H., M. Bell, U. Sreenivasan, H. Hu, J. Liu, K. Dalen, C. Londos, T. Yamaguchi, M. A. Rizzo, R. Coleman, et al. 2011. Unique regulation of adipose triglyceride lipase (ATGL) by perilipin 5, a lipid droplet-associated protein. *J. Biol. Chem.* **286:** 15707–15715.
25. Luo, J., Z. L. Deng, X. Luo, N. Tang, W. X. Song, C. J. Hen, K. A. Sharff, H. H. Luu, R. C. Haydon, K. W. Kinzler, et al. 2007. A protocol for rapid generation of recombinant adenoviruses using the AdEasy system. *Nat. Protoc.* **2:** 1236–1247.
26. McDowell, E. M., and B. F. Trump. 1976. Histologic fixatives suitable for diagnostic light and electron microscopy. *Arch. Pathol. Lab. Med.* **100:** 405–414.
27. Durgan, D. J., M. A. Hotze, T. M. Tomlin, O. Egbejimi, C. Graveleau, E. D. Abel, C. A. Shaw, M. S. Bray, P. E. Hardin, and M. E. Young. 2005. The intrinsic circadian clock within the cardiomyocyte. *Am. J. Physiol. Heart Circ. Physiol.* **289:** H1530–H1541.
28. Durgan, D. J., J. K. Smith, M. A. Hotze, O. Egbejimi, K. D. Cuthbert, V. G. Zaha, J. R. Dyck, E. D. Abel, and M. E. Young. 2006. Distinct transcriptional regulation of long-chain acyl-CoA synthetase isoforms and cytosolic thioesterase 1 in the rodent heart by fatty acids and insulin. *Am. J. Physiol. Heart Circ. Physiol.* **290:** H2480–H2497.
29. Cantó, C., Z. Gerhart-Hines, J. N. Feige, M. Lagouge, L. Noriega, J. C. Milne, P. J. Elliott, P. Puigserver, and J. Auwerx. 2009. AMPK regulates energy expenditure by modulating NAD+ metabolism and SIRT1 activity. *Nature.* **458:** 1056–1060.
30. Muoio, D. M., K. Seefeld, L. A. Witters, and R. A. Coleman. 1999. AMP-activated kinase reciprocally regulates triacylglycerol synthesis and fatty acid oxidation in liver and muscle: evidence that sn-glycerol-3-phosphate acyltransferase is a novel target. *Biochem. J.* **338:** 783–791.
31. Li, L. O., D. G. Mashek, J. An, S. D. Doughman, C. B. Newgard, and R. A. Coleman. 2006. Overexpression of rat long chain acyl-coa synthetase 1 alters fatty acid metabolism in rat primary hepatocytes. *J. Biol. Chem.* **281:** 37246–37255.
32. Bligh, E. G., and W. J. Dyer. 1959. A rapid method of total lipid extraction and purification. *Can. J. Biochem. Physiol.* **37:** 911–917.
33. Haemmerle, G., R. Zimmermann, M. Hayn, C. Theussl, G. Waeg, E. Wagner, W. Sattler, T. M. Magin, E. F. Wagner, and R. Zechner. 2002. Hormone-sensitive lipase deficiency in mice causes diglyceride accumulation in adipose tissue, muscle, and testis. *J. Biol. Chem.* **277:** 4806–4815.
34. Suzuki, J., M. Ueno, M. Uno, Y. Hirose, Y. Zenimaru, S. Takahashi, J. I. Osuga, S. Ishibashi, M. Takahashi, M. Hirose, et al. 2009. Effects of hormone-sensitive lipase-disruption on cardiac energy metabolism in response to fasting and refeeding. *Am. J. Physiol. Endocrinol. Metab.* **297:** E1115–E1124.
35. Dalen, K. T., T. Dahl, E. Holter, B. Arntsen, C. Londos, C. Sztalryd, and H. I. Nebb. 2007. LSDP5 is a PAT protein specifically expressed in fatty acid oxidizing tissues. *Biochim. Biophys. Acta.* **1771:** 210–227.
36. Bell, M., H. Wang, H. Chen, J. C. McLenithan, D. W. Gong, R. Z. Yang, D. Yu, S. K. Fried, M. J. Quon, C. Londos, et al. 2008. Consequences of lipid droplet coat protein downregulation in liver cells: abnormal lipid droplet metabolism and induction of insulin resistance. *Diabetes.* **57:** 2037–2045.
37. Rapaport, D. 2003. Finding the right organelle. Targeting signals in mitochondrial outer-membrane proteins. *EMBO Rep.* **4:** 948–952.
38. Hocsak, E., B. Racz, A. Szabo, L. Mester, E. Rapolti, E. Pozsgai, S. Javor, S. Bellyei, F. Gallyas, Jr., B. Sumegi et al. 2010. TIP47 protects mitochondrial membrane integrity and inhibits oxidative-stress-induced cell death. *FEBS Lett.* **584:** 2953–2960.
39. Novikoff, A. B., P. M. Novikoff, O. M. Rosen, and C. S. Rubin. 1980. Organelle relationships in cultured 3T3-L1 preadipocytes. *J. Cell Biol.* **87:** 180–196.
40. Sturmey, R. G., P. J. O'Toole, and H. J. Leese. 2006. Fluorescence resonance energy transfer analysis of mitochondrial:lipid association in the porcine oocyte. *Reproduction.* **132:** 829–837.
41. Binns, D., T. Januszewski, Y. Chen, J. Hill, V. S. Markin, Y. Zhao, C. Gilpin, K. D. Chapman, R. G. Anderson, and J. M. Goodman. 2006. An intimate collaboration between peroxisomes and lipid bodies. *J. Cell Biol.* **173:** 719–731.
42. Jägerström, S., S. Polesie, Y. Wickström, B. R. Johansson, H. D. Schröder, K. Højlund, and P. Boström. 2009. Lipid droplets interact with mitochondria using SNAP23. *Cell Biol. Int.* **33:** 934–940.
43. Yamaguchi, T., S. Matsushita, K. Motojima, F. Hirose, and T. Osumi. 2006. MLDP, a novel PAT family protein localized to lipid droplets and enriched in the heart, is regulated by peroxisome proliferator-activated receptor alpha. *J. Biol. Chem.* **281:** 14232–14240.
44. Wolins, N. E., B. K. Quaynor, J. R. Skinner, A. Tzekov, M. A. Croce, M. C. Gropler, V. Varma, A. Yao-Borengasser, N. Rasouli, P. A. Kern, et al. 2006. OXPAT/PAT-1 is a aPPAR-induced lipid droplet protein that promotes fatty acid utilization. *Diabetes.* **55:** 3418–3428.
45. Granneman, J. G., H. P. Moore, E. P. Mottillo, Z. Zhu, and L. Zhou. 2011. Interactions of perilipin-5 (Plin5) with adipose triglyceride lipase. *J. Biol. Chem.* **286:** 5126–5135.
46. Granneman, J. G., H. P. Moore, E. P. Mottillo, and Z. Zhu. 2009. Functional interactions between Mldp (LSDP5) and Abhd5 in the control of intracellular lipid accumulation. *J. Biol. Chem.* **284:** 3049–3057.
47. Wolins, N. E., D. L. Brasaemle, and P. E. Bickel. 2006. A proposed model of fat packaging by exchangeable lipid droplet proteins. *FEBS Lett.* **580:** 5484–5491.
48. Skinner, J. R., T. M. Shew, D. M. Schwartz, A. Tzekov, C. M. Lepus, N. A. Abumrad, and N. E. Wolins. 2009. Diacylglycerol enrichment of endoplasmic reticulum or lipid droplets recruits perilipin 3/TIP47 during lipid storage and mobilization. *J. Biol. Chem.* **284:** 30941–30948.
49. Stone, S. J., M. C. Levin, P. Zhou, J. Han, T. C. Walther, and R. V. Jr. Farese. 2009. The endoplasmic reticulum enzyme DGAT2 is found in mitochondria-associated membranes and has a mitochondrial targeting signal that promotes its association with mitochondria. *J. Biol. Chem.* **284:** 5352–5361.
50. Zimmermann, R., J. G. Strauss, G. Haemmerle, G. Schoiswohl, R. Birner-Gruenberger, M. Riederer, A. Lass, G. Neuberger, F. Eisenhaber, A. Hermetter, et al. 2004. Defective lipolysis and altered energy metabolism in mice lacking ATGL. *Science.* **306:** 1383–1386.
51. Wölkart, G., A. Schrammel, K. Dörffel, G. Haemmerle, R. Zechner, and B. Mayer. 2011. Cardiac dysfunction in adipose triglyceride lipase deficiency: treatment with a PPARα agonist. *Br. J. Pharmacol.* Epub ahead of print. May 17, 2011; doi:10.1111/j.1476-5381.2011.01490.x.
52. Schweiger, M., A. Lass, R. Zimmermann, T. O. Eichmann, and R. Zechner. 2009. Neutral lipid storage disease: genetic disorders caused by mutations in ATGL/PNPLA2 or CGI-58/ABHD5. *Am. J. Physiol. Endocrinol. Metab.* **297:** E289–E296.
53. Wang, H., and C. Sztalryd. 2011. Oxidative tissue: perilipin 5 links storage with the furnace. *Trends Endocrinol. Metab.* **22:** 197–203.